Carbohydrate Polymers 76 (2009) 110–116

Contents lists available at ScienceDirect

Carbohydrate Polymers

journal homepage: www.elsevier.com/locate/carbpol

Preparation of nano-sized starch particles by complex formation with *n*-butanol

Jong-Yea Kim, Seung-Taik Lim *

School of Life Sciences and Biotechnology, Korea University, 5-1, Anam-dong, Sungbuk-ku, Seoul 136-701, Republic of Korea

ARTICLE INFO

Article history:
Received 2 June 2008
Received in revised form 12 August 2008
Accepted 25 September 2008
Available online 10 October 2008

Keywords:
Amylose
n-Butanol
Complex
Starch
Nano-crystals

ABSTRACT

High amylose corn starch was dissolved in an aqueous dimethyl sulfoxide solution and allowed to form complexes by migrating gravimetrically into *n*-butanol layer through a membrane filter at 70 °C. The starch–butanol complex yielded V6I-type crystals with broad reflections at d-spacings of 0.657 and 0.446 nm under an X-ray diffractogram. The amylose, the average Mw of which was 2.69×10^5 as determined by size-exclusion column chromatography, mostly contributed to complex formation. Platelets of an average length less than 100 nm, interspersed in amorphous matrices, were observed in the crude complex. By hydrolyzing the crude complex with α-amylase, amorphous matrices were removed and starch crystallites of 10–20 nm, showing a V6I X-ray diffraction pattern at d-spacings 1.187, 0.685, 0.448 and 0.394 nm, were obtained. The average chain length of starch residing in the crystalline complex was DP 9, indicating that single crystallite units consisted of approximately 1.5 helical turn of anhydroglucose chains.

1. Introduction

Amylose, a relatively linear glucan with principally α-(1,4) linkages is capable of complexing with a variety of hydrophobic ligands, leading to a crystal formation, commonly called V-amylose complexes. Depending on the guest compounds such as iodine, dimethyl sulfoxide (DMSO), potassium hydroxide, potassium bromide, aroma compounds, lipids and linear alcohols, different types of V-amylose complexes are produced (Bluhm & Zugenmaier, 1981; Booy & Chanzy, 1979; Godet, Bouchet, Colonna, Gallant, & Bluéon, 1996; Godet, Buléon, Tran, & Colonna, 1993a; Godet, Tran, Delage, & Buléon, 1993b; Helbert & Chanzy, 1994; Jouquand, Ducruet, & Bail, 2006; Nuessli, Putaux, Bail, & Buléon, 2003; Rondeau-Mouro, Bail, & Buléon, 2004). V-amylose structure and thermal characteristics have been investigated mainly by X-ray or electron diffraction (Bluhm & Zugenmaier, 1981; Rappenecker & Zugenmaier, 1981; Sarko & Biloski, 1980; Senti & Witnauer, 1952), and by differential scanning calormetery (DSC) (Bail, Rondeau, & Buléon, 2005; Jouquand et al., 2006; Nuessli et al., 2003), respectively. V-amylose complexes have crystalline structure which can be isolated as hexagonal, rectangular or square platelets (Helbert & Chanzy, 1994) and polycrystalline powders. Most of the complexes consist of crystallites interspersed among amorphous matrices (Godet et al., 1996). With linear alcohols or lipids, amylose forms left-handed single helices consisting of six D-glycosyl units per turn with a pitch of 0.805 nm (V6 complex) (Rappenecker & Zugenmaier, 1981). For the V6 complexes, three types that differ in packing (V6-I, V6-II and V6-III) can be obtained depending on the nature of the guest. In V6-I complexes, guest molecules are entrapped only in the cavity of the helix, whereas in V6-II and V6-III complexes, the molecules are entrapped also in the space between the helices (Brisson, Winter, & Chanzy, 1991; Buléon, Delage, Brisson, & Chanzy, 1990; Helbert & Chanzy, 1994).

Complex formation is substantially retarded by amylolysis, but the complexes formed are resistant to the amylolysis (Cui & Oates, 1999; Czuchajowska, Sievert, & Pomeranz, 1991; Gelders, Duyck, Goesaert, & Delcour, 2005; Godet et al., 1996; Guraya, Kadan, & Champagne, 1997; Heinemann, Zinsli, Renggli, Escher, & Conde-Petit, 2005; Kitahara, Suganuma, & Nahahama, 1996). When crystalline amylose–lipid complexes are treated with a hydrolytic enzyme, amorphous regions on the surface of lamellar crystalline amylose helices may be hydrolyzed initially (Heinemann et al., 2005). It was reported that the enzymatic removal of the amorphous matrices in a V-amylose complex increased the crystallinity (Gelders et al., 2005). On the other hand, a decrease in crystallinity after enzymatic hydrolysis has been observed with a polymorphic transition from V to B-type (Godet et al., 1996). In some cases, the crystallinity is not changed by amylolysis, except for broadening of some diffraction peaks (Seneviratne & Biliaderis, 1991). These results suggest that crystalline regions of amylose complexes may also be disrupted by hydrolysis.

Small-sized starch granules or particles have attracted attention because of their novel physical properties, which include the capability of holding various sensitive materials such as food flavors (Tari, Annapure, Singhal, & Kulkarni, 2003). Also small starch granules can mimic lipid micelles, providing a fat-like texture (Dang & Copeland, 2003). Nano-scale starch particles composed of platelet

* Corresponding author. Tel.: +82 2 3290 3435; fax: +82 2 921 0557.
E-mail addresses: tvand@paran.com (J.-Y. Kim), limst@korea.ac.kr (S.-T. Lim).

0144-8617/$ - see front matter © 2008 Elsevier Ltd. All rights reserved.
doi:10.1016/j.carbpol.2008.09.030

crystallites (20–40 nm long and 15–30 nm wide) have been obtained from waxy maize starch using a selective acid hydrolysis (Putaux, Molina-Boisseau, Momaur, & Dufresne, 2003). The nano-sized starch particles were considered as potential fillers for natural rubber because of their increased reinforcing effect (Angellier, Molina-Boisseau, & Dufresne, 2005). By selective enzymatic hydrolysis, nano-scale starch particles with average diameters of 500 nm were prepared form waxy rice starch (Kim & Lim, 2008). Preparation of the nano-scale starch particles having crystallinity is feasible because the starch granule is inherently composed of nano-scale crystalline blocklets, in a range of diameters from 20 to 500 nm depending on its botanical origin and the location in granule (Gallant, Bouche, & Baldwin, 1997). Therefore, the nano-scale starch particles obtained from acidic or enzymatic hydrolysis consist mainly of the blocklets (Kim & Lim, 2008; Putaux et al., 2003). However, no study has been performed in preparation of the nano-scale starch particles by complex formation with other components.

In this study, starch nano-particles were prepared by complex formation using high amylose maize starch and *n*-butanol, and subsequent enzymatic hydrolysis. The morphology and crystalline characteristics of the starch particles were investigated.

2. Materials and methods

2.1. Materials

An amylomaize starch (Hylon VII, 70% amylose) was provided form National Starch and Chemical Company (Bridgewater, NJ, USA). Porcine pancreatic alpha-amylase (EC 3.2.1.1, activity 1122 units/mg) was purchased from Sigma-Aldrich Company (St. Louis, MO, USA).

2.2. Preparation of nano-sized starch particle

The amylomaize starch (0.5%, w/v) was dispersed in 90% aqueous DMSO solution with heating and stirring in a boiling water bath for 1 h, and then magnetic-stirred at room temperature for 24 h. An aliquot (300 mL) of the starch solution was placed in the upper compartment of a glass filtration apparatus (Millipore, Billerica, MA, USA), and allowed to gravimetrically pass through a membrane filter (PTEE, 10 μm pore size, 47 mm diameter, Millipore, MA, USA) into the bottom compartment filled with *n*-butanol. The filtration apparatus was kept at 70 °C in a convection oven for 6 days. The precipitate in the butanol layer was collected by centrifugation (3390 *g*, 10 min), and then washed three times (50 mL × 3) in the *n*-butanol. The starch remaining in the upper compartment was also quantified by using the phenol-sulfuric acid method (Dubois, Gilles, Hamilton, Rebers, & Smith, 1954).

2.3. DSMO and n-butanol analyses

During complex formation, the solvent (DMSO and *n*-butanol) concentrations in the upper compartment were measured using a high performance liquid chromatography (HPLC). Aliquots of the starch–DMSO solution were taken at regular intervals, and diluted (1/100) with H_3PO_4 solution (0.1% v/v) for HPLC analysis. The HPLC system consisted of a pump (Varian Prostar 210, Varian, Palo Alto, CA, USA), an injector with a 20 μL loop, a column (Supelcogel TM C-610H, 7.8 × 300 mm, Sigma–Aldrich Company, St. Louis, MO), and a refractive index detector (Shodex RI-71, Tokyo, Japan). Column temperature was 50 °C and the mobile phase was 0.1% H_3PO_4 solution (Lee, Lee, & Yoon, 2004) filtered through 0.1 μm cellulose acetate filters (Whatman, UK).

2.4. Alpha-amylolysis of starch–butanol complex

The starch–butanol complex (100 mg, dry basis) was dispersed in water (20 mL), and then an aliquot (0.2 mL) of alpha-amylase solution (5610 units/mL) was added. The mixture was incubated at 25 °C for 60 min with shaking at 170 rpm. Aliquots (10 mL each) of the solution were taken at regular intervals and mixed with ethanol (80 mL) to inactivate the enzyme. After centrifugation (11,325 g for 30 min), the starch complex was recovered and washed three times with 80% ethanol (50 mL × 3). The total carbohydrate content in the supernatant was also measured to determine the degree of amylolysis by using the phenol-sulfuric acid method (Dubois et al., 1954).

2.5. Transmission electron microscopy (TEM)

The starch–butanol complex isolated as particles (0.3 mg) was suspended in ethanol (1 mL) and a drop of the suspension was deposited on a formvar-coated microscopy grid. It was negatively stained with a drop of 2% (w/v) uranyl acetate, dried at room temperature, and observed using a transmission electron microscope (Philips Tecnai 12, Eindhoven, Netherlands).

2.6. Particle size distribution

Particle size distribution of the starch complexes was determined in water by using a dynamic light scattering detector (Dynapro Titan, Wyatt Technology, Santa Barbara, CA). The refractive index and the viscosity of water provided by the calculation software were 1.333 and 1.00 cP at 20 °C, respectively.

2.7. X-ray diffraction pattern

The crystallinity of the starch complex particles was determined by using an X-ray diffractometer (MAC Science Co., Japan) at a target voltage and current of 40 kV and 40 mA, respectively. The scanning range and rate were 3–30° (2θ) and 2.0°/min, respectively.

2.8. Differential scanning calorimetry (DSC)

Thermal analyses of the starch complexes were carried out by using a differential scanning calorimeter (Seiko DSC 6100, Chiba, Japan). Starch particles (2.0 mg) and water (4.0 mg) were mixed in an aluminum DSC pan, and then the mixture was equilibrated at 4 °C for 2 h. The scanning was from 0 to 150 °C at a heating rate of 5 °C/min, with a reference of an empty pan.

2.9. Molecular size of starch chains

The molecular size of the starch chains in the complex, before and after amylolysis, was measured by using a high-pressure size-exclusion chromatography (HPSEC, TSK G5,000 PWXL and TSK G3,000 PWXL Montgomeryville, PA, USA) and a refractive index detector (Shodex RI-71, Tokyo, Japan). The starch–butanol complex (2 mg, dry basis) was dissolved in 1 N NaOH solution (1 mL) by vortexing, and the solution was diluted by adding 50 mM $NaNO_3$ (3 mL). After neutralizing with 1 M HCl (1 mL), the solution was autoclaved (121 °C) for 20 min for complete dissolution, and then filtered through a porous membrane filter (5.0 μm, Pall Gelman Sciences, Ann Arbor, MI, USA). Dextran standards of different molecular weights (2000,000, 500,000, 112,000 and 40,000) and pullulan standards (47,300, 22,800, 5900 and 667) were used to measure the molecular weights of the starch and starch dextrins resulting from the amylolysis. A semi-logarithmic plot of the standard molecular weights versus K_{av} at the maximum

refractive index value for pullulan standards was used for the molecular weight calculation.

The HPSEC system consisted of a pump (Varian Prostar 210, Varian, Palo Alto, CA, USA.), an injector with 1 mL loop and HPSEC columns. The mobile phase was 50 mM $NaNO_3$ solution containing 0.02% NaN_3, and the flow rate was 0.4 mL/min.

3. Results

3.1. Formation of starch nano-particles

During the period of complex formation between starch and *n*-butanol in a filtration apparatus (70 °C, for 6 days), DMSO and butanol diffused into the adjacent compartment through the membrane filter. Major force for the solvent migration was the gravimetric transfer of the DMSO solution containing starch down into the *n*-butanol layer. The changes in DMSO and *n*-butanol concentrations in the upper compartment are presented in Fig. 1. DMSO content gradually decreased, whereas the butanol content increased as a result of solvent diffusion. However, solvent migration became retarded after 72 h and reached equilibrium in 4 days of the storage. The equilibrium concentrations for DMSO and *n*-butanol in the upper compartment were 57 and 37%, respectively. As the solvent profile indicates, starch migration also became minimal after 72 h.

The starch concentration in the upper compartment constantly decreased during storage for complex formation as shown in Fig. 1, indicating that the starch migrated into the *n*-butanol layer. Up to 72 h, it decreased only slightly, but its concentration dropped rapidly afterward. This result was unexpected because the rate of solvent migration decreased after 72 h. The sudden drop of starch concentration was caused by the precipitation of starch on the membrane filter induced by the *n*-butanol diffused up into the DMSO solution. It was also expected that complex formation with butanol might be somewhat hindered as DMSO concentration in the butanol layer increased. Therefore, complex formation might occur very slowly as the two solvents were spontaneously mixed. The butanol layer in which the complex formation occurred gradually became hazy during storage, and precipitates of the complex were observed after 6 h. The starch maximally precipitated in the *n*-butanol layer after 72 h was 6.78% based on the initial amount used. During the complex formation, there was no significant change in volumes of both layers, indicating that the consumption of *n*-butanol for complex formation was very small.

The starch–butanol complex was isolated as the precipitate, and subjected to amylolysis. In the hydrolysis profile (Fig. 2), the starch in the complex was rapidly hydrolyzed within 20 min, but remained relatively stable afterward. During the rapid hydrolysis that occurred in the first 20 min, most of the starch (85.46%) was hydrolyzed. Therefore only about 15% of the starch that complexed with butanol remained unhydrolyzed.

3.2. Morphology and particle size

Fig. 3 shows the TEM images of the starch–butanol complexes, before and after enzymatic hydrolysis. Prior to the hydrolysis, the starch complex contained polygonal platelets interspersed in the matrix (Fig. 3a). The platelets had shapes similar to those reported for an amylose–*n*-butanol complex (Booy & Chanzy, 1979; Manley, 1964), but their length was less (<100 nm) than that in the report. By amylolysis for 60 min, most of the matrix surrounding the platelets was removed, and the sphere or oval shaped nano-particles were observed as clusters (Fig. 3b). The platelets contained portions of starch chains complexed with butanol, which were selectively hydrolyzed by the enzyme, and it revealed the crystallite particles in relatively uniform size (10–20 nm diameters as

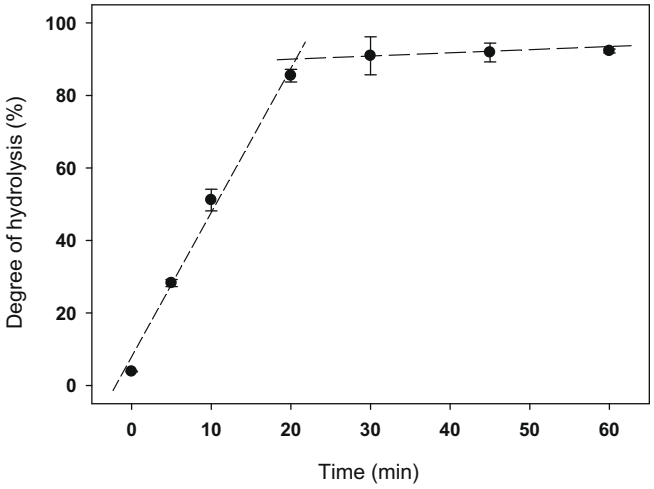

Fig. 2. Enzymatic hydrolysis profile of the starch–butanol complex recovered from the butanol layer.

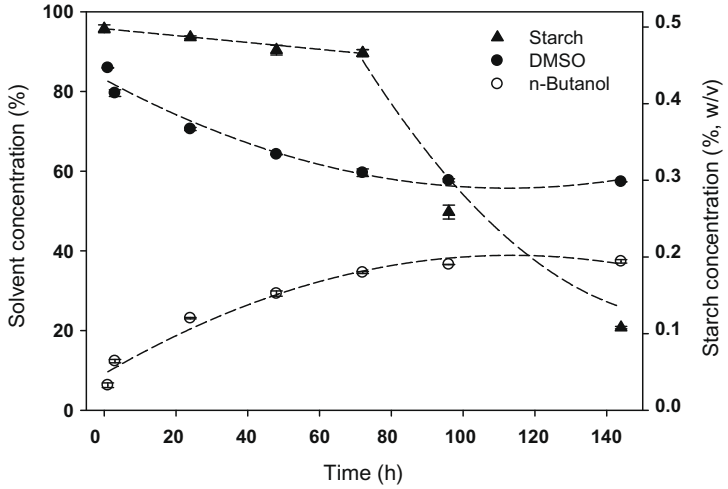

Fig. 1. Changes in DMSO, *n*-butanol and starch concentrations in the upper compartment during complex formation.

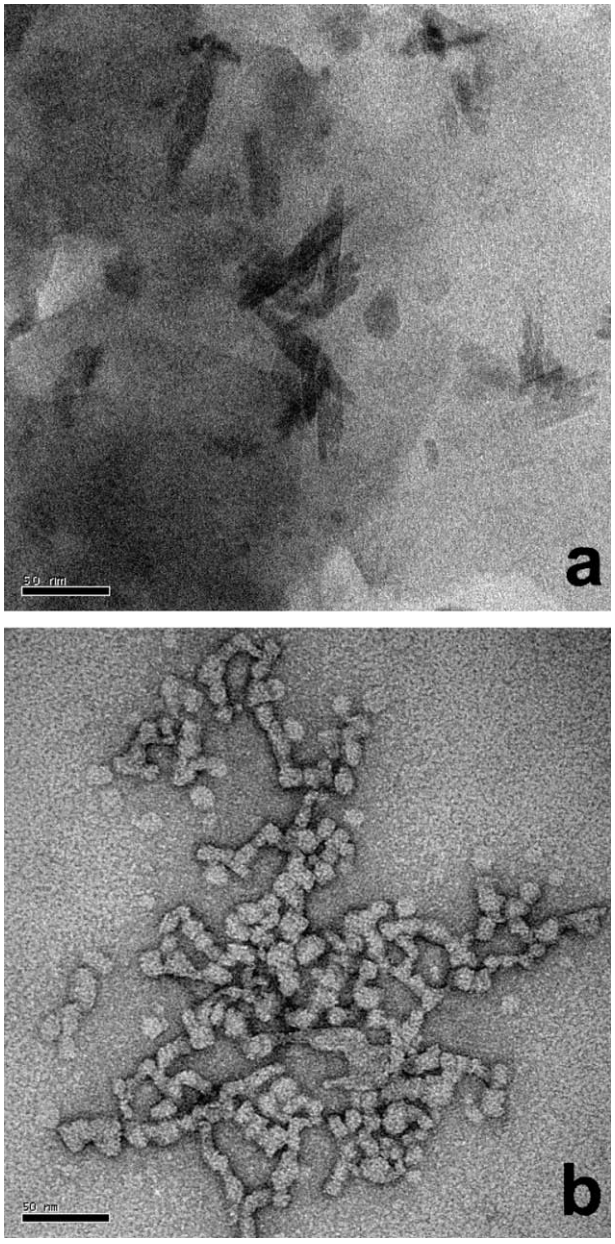

Fig. 3. TEM micrographs of negatively stained starch–butanol complexes: (a) crude complex formed in butanol layer (72 h), (b) isolated complex by enzymatic hydrolysis (60 min).

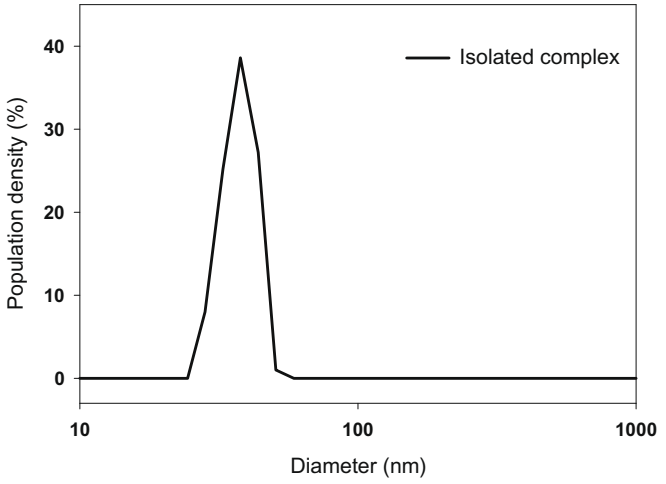

Fig. 4. Particle size distribution of the starch complex isolated after enzymatic hydrolysis.

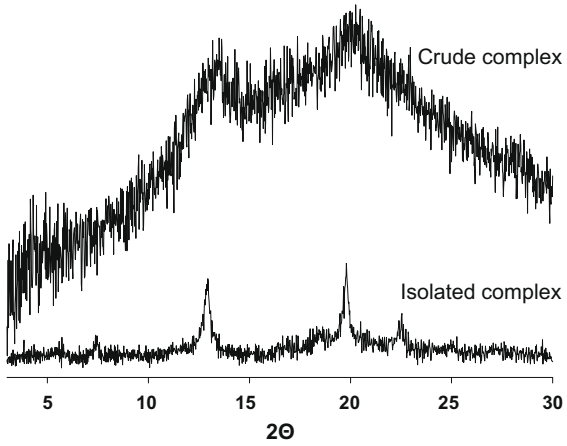

Fig. 5. X-ray diffraction patterns of the crude and isolated starch complexes.

shown in Fig. 3b). Because the TEM observation was made with the dried samples, the aggregation of the particles was considered as a natural phenomenon.

The size distribution of the starch complex particles isolated after the amylolysis is present in Fig. 4, showing that the starch particles were exclusively in a size range of diameter from 28 to 51 nm.

3.3. X-ray diffraction (XRD)

X-ray diffraction patterns of the complex particles are presented in Fig. 5. Before the enzymatic hydrolysis, the particles yielded a V6-I type XRD pattern with two broad reflections at d-spacings 0.657 and 0.446 nm (13.08 and 19.78° 2θ). However, the XRD diagram revealed that the crystallinity was only partial with an overlapping amorphous background. The starch nano-particles isolated by the enzymatic hydrolysis also exhibited a V6-I type XRD pattern with four sharp reflections at d-spacings 1.187, 0.685, 0.448 and 0.394 nm (7.44, 12.91, 19.79 and 22.54° in 2θ). The XRD revealed that the α-amylolysis occurred mainly in the amorphous region of the complex, leaving the crystalline nano-particles (Gelders et al., 2005).

3.4. Differential scanning calorimetry (DSC)

Crystal melting characteristics of the starch–butanol complex measured using a DSC is shown in Table 1. Melting of V-amylose is reversible but its characteristics such as temperature range and enthalpy depend on crystallization conditions (Bail et al., 2005). The endothermic transition of a typical V-amylose was observed for the crude starch–butanol complex, but melting enthalpy of the complex was low (0.40 J/g). Melting enthalpy of the complexes, however, increased dramatically (0.40 → 13.55 J/g) by the α-amylolysis, confirming the XRD result that the amorphous part of the complex was removed by the enzymatic hydrolysis. The onset temperature for melting was decreased, but overall melting range was increased by the hydrolysis. Melting of both crude and isolated complexes appeared highly reversible, which is typical for the V-amylose complexes (Bail et al., 2005).

Table 1
Crystal melting properties of the crude and isolated starch complexes.

Samples	Melting temperatures[a]			Melting enthalpy
	T_o (°C)	T_p (°C)	T_c (°C)	ΔH (J/g)
Crude complex	87.10 ± 0.55	91.10 ± 0.26	94.00 ± 0.13	0.40 ± 0.14
Second scan	87.20 ± 0.74	90.90 ± 0.61	94.00 ± 0.29	0.39 ± 0.13
Isolated starch complex	72.33 ± 0.25	89.90 ± 1.13	101.03 ± 0.86	13.55 ± 0.43
Second scan	78.50 ± 0.40	95.97 ± 0.25	104.70 ± 0.75	13.45 ± 0.16

[a] T_o, T_p and T_c are the onset, peak and conclusion temperatures, respectively.

3.5. Molecular size of starch chains

Molecular size distributions of the high amylose maize starch and starch complexed with butanol before and after amylolysis are shown in Fig. 6a. The starch complexed with butanol prior to the amylolysis (crude complex in Fig. 6) consisted mainly of amylose, although some amylopectin was found. Amylopectin was expected to be more difficult to pass through the membrane filter than amylose due to its larger size. The amylopectin molecules migrated to the butanol compartment, if any, were less capable of forming the complex with butanol than amylose molecules. Therefore, the amylopectin migrated in the butanol compartment might be recovered mainly in the amorphous matrix of the complex (Fig. 3).

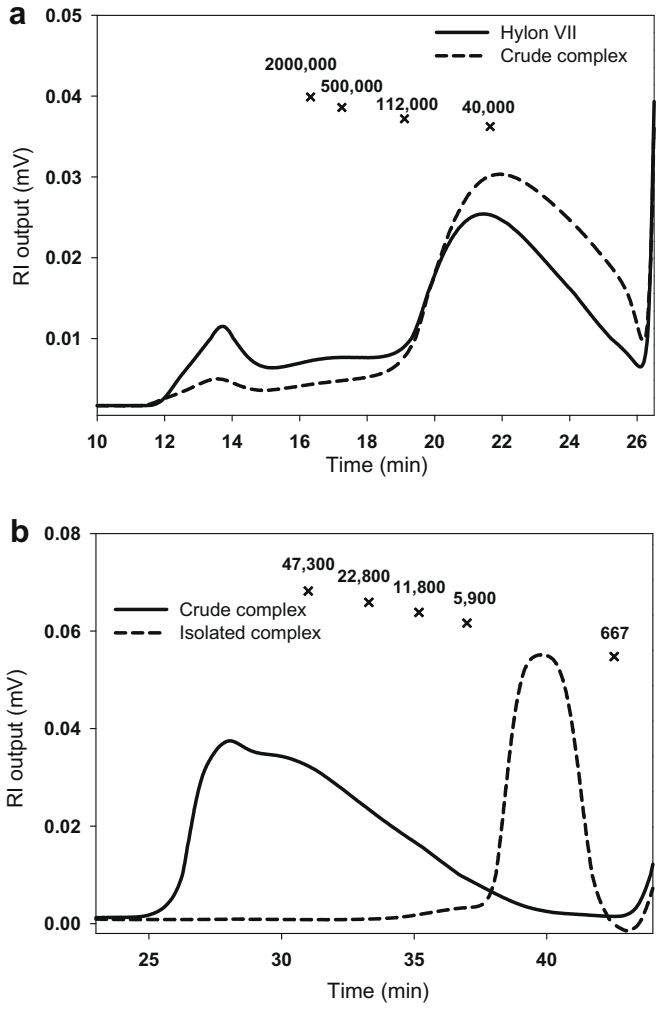

Fig. 6. Molecular weight distribution of high amylose corn starch (Hylon VII), and starch complexes.

The molecular size of starch isolated from the crude complex after the amylolysis is present in Fig. 6b. Due to the excessive level of hydrolysis (60 min), the starch was heavily hydrolyzed and became dextrins of dramatically reduced molecular weight (about 1.5 K). It is noteworthy that the molecular size of the dextrin was very uniform (low polydispersity). The size of dextrin in the isolated complex was equivalent to a degree of polymerization (DP) of approximately 9. Because six anhydroglucose units make one helical turn in the V-6 complex, the nano-particles isolated from starch–butanol complexes consist of no more than one helical turn.

4. Discussion

Preparation of nano-sized starch particles was possible by formation of the starch–*n*-butanol complex. A viscous DMSO solution containing starch sample, separated from butanol by a membrane filter, migrated into the butanol layer by gravimetric force, and migration rate of starch molecules could be controlled by using the membrane of proper pore size. Amylose rather than amylopectin was more favored in the complex formation because of its linearity and mobility, and it was confirmed by size-exclusion column chromatography (Fig. 6a). The structural development into crystallites from the complex was possible as both solvents were diffused slowly through the membrane. The rate-controlled system allowed amylose chains to form the V-amylose complex having good crystallinity, rather than B-type crystals or amorphous aggregates that often resulted from direct contact of starch to alcohol. The mild heating (70 °C in this case) allowed amylose chains remaining mobile, and assisted transfer of amylose through the membrane.

During complex formation, the migration of DMSO and butanol through the membrane filter proceeded until 72 h, and reached equilibrium after about 40% exchange. It was believed that there were gradients between DMSO and butanol formed in the vicinity of the membrane. If the amount of butanol in the mixture was not sufficient, starch could not form the complex. It was found that when the volume of butanol compartment was less than 150 mL, the starch complex was not formed in the experimental conditions (data not shown). Therefore, it was supposed that the starch, mostly amylose, should migrate into the region where butanol concentration was high enough in order that the complex formation occurred readily.

It was reported that V-amylose was formed as polycrystalline powders interspersed in amorphous matrices (Godet et al., 1996). Alcohol-amylose complex appeared platelet-like, regardless of alcohol chain length (Whittam, Orford, Ring, Clark, Parker, Cairns, & Miles, 1989). When *n*-butanol formed a complex with amylose, the rectangular platelets had a length of approximately larger than 1 μm (Booy & Chanzy, 1979; Manley, 1964). The complex isolated in the butanol solution showed similar morphology in which platelet-like crystallites were interspersed in amorphous matrices (Fig. 3a). However, the size of the complex crystals was smaller (<100 nm) than those reported (Buléon et al., 1990; Nuessli et al., 2003). Considering that each platelet is a polycrystalline assembly, its size could readily vary according to the physical environmental conditions. Because the crystalline complexes have high resistance to enzymatic hydrolysis, whereas amorphous matrices are easily hydrolyzed (Biais, Bail, Robert, Pontoire, & Buléon, 2006; Cui & Oates, 1999; Godet et al., 1996), the crystalline complexes could be recovered by enzymatic hydrolysis. The hydrolysis pattern of the complex has been reported by several researches (Cui & Oates, 1999; Gelders et al., 2005), but the maximum degree of hydrolysis of the complex in this study was higher than those in the literature (Fig. 2). We assume that the complexes prepared in this experi-

ment contained a larger percentage of amorphous regions, not only as continuous amorphous matrices but even inside the platelets. XRD patterns confirmed the presence of a large amorphous portion in the crude complex that could be removed effectively by α-amylolysis (Fig. 5). The increase of crystal melting enthalpy after α-amylolysis (Table 1) supported the hypothesis that the amorphous regions in the complex were selectively hydrolyzed.

Amylose may form complexes with *n*-butanol in V6-II type crystals, in which butanol is entrapped not only within the helices but in the space between the helices (Bail et al., 2005; Helbert & Chanzy, 1994) and thus drying V6-II amylose to remove *n*-butanol between helices may transform it to V6-I-amylose (Bail et al., 2005). However, the complex prepared in this study yielded only V6-I crystals as confirmed by XRD patterns (Fig. 5). The absence of butanol between the helices might influence the size of the unit cells (Helbert & Chanzy, 1994). During crude complex formation in the butanol layer, *n*-butanol was entrapped inside the amylose helices, not between helices. The complex formation in this system started at the contact of starch with butanol, right after the migration through the membrane, and only limited butanol was incorporated in the complex formation. This system was different from the complex formation in a batch-type mixture or starch solution and butanol in which the complex was formed with butanol incorporated between helices.

From the crude complex which had been formed in bulky clusters, starch nano-particles, therefore, could be obtained by selective α-amylolysis in the amorphous matrices. The starch nano-particles isolated revealed crystallites of spherical or oval crystallites, with a diameter range of approximately 10–20 nm (Fig. 3). The enzymatic removal of the amorphous matrices caused the change in their morphology. It was reported that V-amylose has a lamellar structure assembled by the lateral stacking of tube-like helices with up and down folding (Brisson et al., 1991; Manley, 1964). Although the stacking may result in dense packing, the enzyme eventually attacked most of the chains which were not involved in crystal formation with butanol, leave only maltodextrins of average DP 9.

Cyclodextrins (CDs), cyclic oligomers consisting of six or more α-1, 4-linked D-glucopyranose units (Saenger, Jacob, Gessler, Steiner, Hoffmann, Sanbe, Koizumi, Smith, & Takaha, 1998) have conical molecular structures with hydrophobic interior and hydrophilic exterior so the internal cavity can include a various guest compound, whereas the hydrophilic exterior helps CDs to be solved in water (Hapiot, Tilloy, & Monflier, 2006). Like CDs, linear maltodextrins could form complexes with various guest compounds as shown in this study. CDs may form aggregates in aqueous solution with the size of about 90–300 nm, depending on the concentration, temperature and pH of aqueous solution (He, Fu, Shen, & Gao, 2008). It was also reported that the inclusion complexes of CDs formed lager aggregates in aqueous solutions than did CDs (Loftsson, Másson, & Brewster, 2004). The nano-particles of maltodextrins and butanol complex prepared by using starch in this study had much smaller size than the aggregates of CDs or CD complexes reported in literatures. More importantly, starch or maltodextrins are more readily available with lower costs compared to CDs, and also have a great versatility in complexing with various guest compounds.

5. Conclusion

Crystalline starch nano-particles could be prepared by complex formation with *n*-butanol and successive enzymatic hydrolysis (amylolysis). Complex formation involved mainly amylose rather than amylopectin. The V6 crystalline structure was properly developed by slow migration of starch and solvents. However, the amylose–butanol complex formed in the butanol layer contained a large portion of amorphous matrices, so that selective removal of these was needed to isolate the nano-particles. The starch nano-particles had spherical or oval shape with diameters 10–20 nm. Starch molecules in the particles had been reduced in size to an average DP of 9. Due to significant loss by hydrolysis (85–90%) of the starch initially complexed, the overall yield of the nano-particles was very low. For large-scale preparation, optimization in the process should be studied. This complex formation process is highly potential in utilizing starch or its dextrins as nano-carriers for small and active components.

References

Angellier, H., Molina-Boisseau, S., & Dufresne, A. (2005). Mechanical properties of waxy maize starch nanocrystal reinforced natural rubber. *Macromolecules, 38*(22), 9161–9170.

Bail, P. L., Rondeau, C., & Buléon, A. (2005). Structural investigation of amylose complexes with small ligands: helical conformation, crystalline structure and thermostability. *International Journal of Biological Macromolecules, 35*(1), 1–7.

Biais, B., Bail, P. L., Robert, P., Pontoire, B., & Buléon, A. (2006). Structural and stoichiometric studies of complexes between aroma compounds and amylose. Polymorphic transitions and quantification in amorphous and crystalline areas. *Carbohydrate Polymers, 66*(3), 306–315.

Bluhm, T. L., & Zugenmaier, P. (1981). Detailed structure of the Vh-amylose–iodine complex: a linear polyiodine chain. *Carbohydrate Research, 89*(1), 1–10.

Booy, F. P., & Chanzy, H. (1979). Electron diffraction study of single crystals of amylose complexed with *n*-butanol. *Biopolymers, 18*(6), 2261–2266.

Brisson, J., Winter, W. T., & Chanzy, H. (1991). The crystal and molecular structure of V_H amylose by electron diffraction analysis. *International Journal of Biological Macromolecules, 13*(1), 31–39.

Buléon, A., Delage, M. M., Brisson, J., & Chanzy, H. (1990). Single crystals of V amylose complexed with isopropanol and acetone. *International Journal of Biological Macromolecules, 12*(1), 25–33.

Cui, R., & Oates, C. G. (1999). The effect of amylose–lipid complex formation on enzyme susceptibility of sago starch. *Food Chemistry, 65*(4), 417–425.

Czuchajowska, Z., Sievert, D., & Pomeranz, Y. (1991). Enzyme-resistant starch. IV. Effects of complexing lipids. *Cereal Chemistry, 68*(5), 537–542.

Dang, J. M. C., & Copeland, L. (2003). Imaging rice grains using atomic force microscopy. *Journal of Cereal Science, 37*(2), 165–170.

Dubois, M., Gilles, K. A., Hamilton, J. K., Rebers, P. A., & Smith, F. (1954). Colorimetric method for determination of sugars and related substances. *Analytical Chemistry, 28*(3), 350–356.

Gallant, D. J., Bouche, B., & Baldwin, P. M. (1997). Microscopy of starch: evidence of a new level of granule organization. *Carbohydrate Polymers, 32*(3), 177–191.

Gelders, G. G., Duyck, J. P., Goesaert, H., & Delcour, J. A. (2005). Enzyme and acid resistance of amylose–lipid complexes differing in amylose chain length, lipid and complexation temperature. *Carbohydrate Polymers, 60*(3), 379–389.

Godet, M. C., Bouchet, B., Colonna, P., Gallant, D. J., & Bluéon, A. (1996). Crystalline amylose–fatty acid complexes: morphology and crystal thickness. *Journal of Food Science, 61*(6), 1196–1201.

Godet, M. C., Buléon, A., Tran, V., & Colonna, P. (1993a). Structural features of fatty acid-amylose complexes. *Carbohydrate Polymers, 21*(2), 91–95.

Godet, M. C., Tran, V., Delage, M. M., & Buléon, A. (1993b). Molecular modelling of the specific interactions involved in the amylose complexation by fatty acids. *International Journal of Biological Macromolecules, 15*(1), 11–16.

Guraya, H., Kadan, R., & Champagne, E. T. (1997). Effect of rice starch–lipid complexes on in vitro digestibility, complexing index, and viscosity. *Cereal Chemistry, 74*(5), 561–565.

Hapiot, F., Tilloy, S., & Monflier, E. (2006). Cyclodextrins as supramolecular hosts for organometallic complexes. *Chemical reviews, 106*(3), 767–781.

He, Y., Fu, P., Shen, X., & Gao, H. (2008). Cyclodextrin-based aggregates and characterization by microscopy. *Micron, 39*(5), 495–516.

Heinemann, C., Zinsli, M., Renggli, A., Escher, F., & Conde-Petit, B. (2005). Influence of amylose-flavor complexation on build-up and breakdown of starch structures in aqueous food model systems. *LWT-Food Science and Technology, 38*(8), 885–894.

Helbert, W., & Chanzy, H. (1994). Single crystals of V amylose complexed with *n*-butanol or *n*-pentanol: structural features and properties. *International Journal of Biological Macromolecules, 16*(4), 207–213.

Jouquand, C., Ducruet, V., & Bail, P. L. (2006). Formation of amylose complexes with C6-aroma compounds in starch dispersions and its impact on retention. *Food Chemistry, 96*(3), 461–470.

Kim, J.-Y., & Lim, S.-T. (2008). Fragmentation of waxy rice starch granules by enzymatic hydrolysis. *Cereal Chemistry, 85*(2), 182–187.

Kitahara, K., Suganuma, T., & Nahahama, T. (1996). Susceptibility of amylose–lipid complexes to hydrolysis by glucoamylase from rhizopus niveus. *Cereal Chemistry, 73*(4), 428–432.

Lee, Y., Lee, C., & Yoon, J. (2004). Kinetics and mechanisms of DMSO (dimethylsulfoxide) degradation by UV/H_2O_2 process. *Water Research, 38*(10), 2579–2588.

Loftsson, T., Másson, M., & Brewster, M. E. (2004). Self-association of cyclodextrin and cyclodextrin complexes. *Journal of Pharmaceutical Sciences, 93*(5), 1091–1099.

Manley, R. J. (1964). Chain folding in amylose crystals. *Journal of Polymer Science Part A, 2*(10), 4503–4515.

Nuessli, J., Putaux, J. L., Bail, P. L., & Buléon, A. (2003). Crystal structure of amylose complexes with small ligands. *International Journal of Biological Macromolecules, 33*(5), 227–234.

Putaux, J. L., Molina-Boisseau, S., Momaur, T., & Dufresne, A. (2003). Platelet nanocrystals resulting from the disruption of waxy maize starch granules by acid hydrolysis. *Biomacromolecules, 4*(5), 1198–1202.

Rappenecker, G., & Zugenmaier, P. (1981). Detailed refinement of the crystal structure of Vh-amylose. *Carbohydrate Research, 89*(1), 11–19.

Rondeau-Mouro, C., Bail, P. L., & Buléon, A. (2004). Structural investigation of amylose complexes with small ligands: inter- or intra-helical associations? *International Journal of Biological Macromolecules, 34*(5), 251–257.

Saenger, W., Jacob, J., Gessler, K., Steiner, T., Hoffmann, D., Sanbe, H., et al. (1998). Structures of the common cyclodextrins and their lager analogues-beyond the doughnut. *Chemical reviews, 98*(5), 1787–1802.

Sarko, A., & Biloski, A. (1980). Crystal structure of the koh-amylose complex. *Carbohydrate Research, 79*(1), 11–21.

Seneviratne, H. D., & Biliaderis, C. G. (1991). Action of alpha-amylase on amylase-lipid complex superstructures. *Journal of Cereal Science, 13*, 129–143.

Senti, R. T., & Witnauer, L. P. (1952). X-ray diffraction studies of addition compounds of amylose with inorganic salts. *Journal of Polymer Science, 9*(2), 115–132.

Tari, T. A., Annapure, U. S., Singhal, R. S., & Kulkarni, P. R. (2003). Starch-based spherical aggregates: screening of small granule sized starches for entrapment of a model flavouring compound, vanillin. *Carbohydrate Polymers, 53*(1), 45–51.

Whittam, M. A., Orford, P. D., Ring, S. G., Clark, S. A., Parker, M. L., Cairns, P., et al. (1989). Aqueous dissolution of crystalline and amorphous amylose–alcohol complexes. *International Journal of Biological Macromolecules, 11*(11), 339–344.